APS physics

CHORUS

This is the accepted manuscript made available via CHORUS. The article has been published as:

Universality in the entropy change for the inverse magnetocaloric effect

Anis Biswas, Sayan Chandra, Tapas Samanta, Barnali Ghosh, Subarna Datta, M. H. Phan, A. K. Raychaudhuri, I. Das, and H. Srikanth

Phys. Rev. B **87**, 134420 — Published 22 April 2013

DOI: 10.1103/PhysRevB.87.134420

Universality in the entropy change for the inverse magnetocaloric effect

Anis Biswas[1, #], Sayan Chandra[1], Tapas Samanta[2,⊥], Barnali Ghosh[3], Subarna Datta[3], M. H. Phan[1], A. K. Raychaudhuri[3], I. Das[2], and H. Srikanth[1, *]

1. Department of Physics, University of South Florida, Tampa, FL 33620, USA
2. Experimental Condensed Matter Physics Division, Saha Institute of Nuclear Physics, Kolkata 700064, India
3. Unit of Nanoscience, S N Bose National Centre for Basic Science, Kolkata 700098, India

Abstract:

A comprehensive study of the temperature (T) and magnetic field (H) dependence of magnetic entropy change (ΔS_M) for different materials exhibiting inverse magnetocaloric effect (IMCE) is reported. We show that ΔS_M follows a power law dependence of H ($\Delta S_M \sim H^n$, n is an exponent) for these compounds. In contrast to conventional magnetocaloric effect (CMCE), n is independent of H and T in the case of IMCE. As a result, a universal master curve can be constructed to describe $\Delta S_M(T)$ of the IMCE systems for different H without rescaling temperature axis. This is completely different from that reported for CMCE, where the rescaling of temperature axis with the introduction of at least one reference temperature is needed for constructing a universal curve. The different universal behavior of IMCE is attributed to the constant value of n in any field and temperature, which is a generic feature of IMCE systems irrespective of their magnetic state and nature of phase transition. From the proposed phenomenological universal curve, one can extrapolate the magnetocaloric properties of IMCE systems in any temperature and magnetic field range, which would be helpful in designing controlled active magnetic refrigeration devices.

Key words: Magnetocaloric, Inverse magnetocaloric, Universal curve

PACS: 75.30.Sg, 75.30.kz

E-mail: anisbiswas@usf.edu
*E-mail: sharihar@usf.edu
⊥ Present address: Southern Illinois University, USA

The study of the magnetocaloric properties of materials has been a subject of extensive research from both fundamental and application points of view[1-5]. Magnetic refrigeration based on the magnetocaloric effect (MCE) is considered to be a viable alternative to conventional gas compression refrigeration technology[1]. Furthermore by investigating magnetocaloric parameters of materials, one can acquire insightful understanding about complex magnetic phases present in the system, which may not be possible by just studying magnetization[6-9].

Generally the application of a magnetic field causes the reduction in magnetic entropy of a refrigerant material and if the material is demagnetized adiabatically in subsequent steps, low temperature can be achieved. However, recent studies have revealed that an inverse effect can occur in some magnetic systems for which a magnetic field induced enhancement in magnetic configuration entropy is observed, and this is known as 'inverse magnetocaloric effect' (IMCE)[10-16]. From a magnetic cooling perspective, it is worth mentioning that the adiabatic magnetization of materials exhibiting IMCE can generate cooling, and the efficiency of a refrigeration device can be improved by utilizing IMCE materials as 'heat-sinks' in composites with conventional magnetic refrigerants[10]. Although IMCE is mostly observed in antiferromagnetic and ferrimagnetic materials, some ferromagnetic systems also show this effect due to martensitic transition [10,14-15].

One of the important issues in studies related to magnetic refrigeration is to understand how the MCE of a material at different temperatures evolves with applied magnetic fields[1]. For instance, a detailed analysis of the field dependence of MCE can provide useful information about the performance of a refrigerant for magnetic field ranges used in actual refrigeration cycles. Beside this, such a study can also be helpful to get deeper understanding of the nature of magnetic phase transitions and phase coexistence in the material[6-9]. The magnetic field dependence of the magnetocaloric parameters has been shown to be associated with the intricate nature of magnetic phase transition and can be parameterized by critical exponents governing the transition[17-21]. Recently, Franco et al. have introduced a method of using 'universal master curve' to describe the temperature dependence of magnetic entropy change [$\Delta S_M(T)$] in different applied magnetic fields for conventional magnetocaloric effect (CMCE)[17,18]. This method is valid when the magnetic transition in the material is of second-order type in nature. According to these studies, all $\Delta S_M(T)$ curves for different applied magnetic fields for a FM system will

collapse onto a universal master curve, when $\Delta S_M(T)$ is normalized to its peak value and temperature axis is rescaled as[17]

$$\theta = (T-T_C)/(T_r-T_C) \qquad (1)$$

with T_r being a reference temperature corresponding to a certain fraction 'f' that satisfies $\Delta S_M(T_r)/ \Delta S_M (T_C) = f$ [17,18]. For systems with co-existence of more than one FM phase, two reference temperatures have to be used in the definition of θ to construct a universal curve[18]. It is found that the construction of universal curve using this method is not valid when CMCE arises due to the first order phase transition[23]. This idea of such universality has been extensively verified for different kinds of ferromagnetic systems showing CMCE as a result of the second order transition and it has also been theoretically well grounded[17-23]. However, little attention has been paid to systems exhibiting IMCE. As the IMCE materials are potentially important components in magnetic refrigeration, it is essential to gain a clear understanding of the temperature and field dependences of ΔS_M in these systems. Most recently, our preliminary study has revealed that a universal behavior can exist in antiferromagnetic systems showing IMCE[24]. That research was only limited to only one class of materials (manganites), and the analysis of the IMCE behavior was confined up to a 3 T magnetic field, below the critical field (3.5 T) at which the first order-like transition occurred for those particular systems[24]. This leads to the emergence of the following important questions that need to be addressed in order to get comprehensive understanding of the universal behavior of IMCE:

(i) Is a universal behavior attributed to the *antiferromagnetic* transition of an IMCE system?

(ii) Can a universal curve be constructed for materials undergoing a first-order structural or magnetic field induced transition?

(iii) Can a similar universal behavior exist in CMCE systems with antiferromagnetic correlation?

(iv) Does a universal curve exist for *ferromagnetic* materials exhibiting IMCE?

The overall aim of this paper is to address these outstanding questions through a systematic study of the magnetocaloric effect and universal behavior in three kinds of magnetic systems: (a) *antiferromagnetic* materials showing IMCE (antiferromagnetic manganites:

$La_{0.17}Ca_{0.83}MnO_3$ and $La_{0.125}Ca_{0.875}MnO_3$); (b) materials showing an antiferromagnetic and ferromagnetic coexistence and CMCE (a self-doped manganite: $LaMnO_{3.04}$); and (c) *ferromagnetic* materials showing IMCE (a representative Heusler alloy: $Ni_{50}Mn_{36}Sn_{14}$).

Polycrystalline samples of $La_{0.17}Ca_{0.83}MnO_3$ and $La_{0.125}Ca_{0.875}MnO_3$ were prepared by using sol-gel technique followed by annealing at 1400 °C for 36 hours[25]. For comparison, we have also extended our study to self-doped $LaMnO_{3.04}$ (LMO), which was prepared by standard solid-state reaction method [9]. The powder X-ray diffraction (XRD) study confirmed the successful preparation of samples. All the three samples are of orthorhombic structure. The XRD patterns of the samples have been shown in Fig. 1. The $Ni_{50}Mn_{36}Sn_{14}$ sample was prepared by the melt-spinning method. The details of the preparation and characterization of this sample have been reported elsewhere[14]. A physical property measurement system (PPMS) equipped with vibrating sample magnetometer (VSM) was used for the magnetization study.

We investigated the temperature dependence of magnetization [M(T)] to probe the magnetic transitions in the samples. From M(T) curves (measured in the presence of 0.02 T magnetic field) for both LCMO-1 and LCMO-2 (inset, Fig. 2a), it is clear that the samples undergo an antiferromagnetic transition at T_N ~ 170 and ~125 K, respectively. There is negligible irreversibility between M(T) curves recorded in zero field cooled and field cooled protocol. The reversibility of M(T) curves can be an indication of the second order nature of phase transition. We have also studied the isothermal magnetic field dependence of magnetization [M(H)] and checked H/M vs. M^2 (Arrott plots) obtained from M(H) curves to get an idea about the nature of magnetic phase transitions in the samples. The representative M(H) curves at some selected temperatures for LCMO-1 and LCMO-2 are shown in Fig. 2a and 2b, respectively. As an example, the Arrott plots for LCMO-2 are given in the inset of Fig. 2b. It appears that the Arrott plots have positive slopes up to magnetic fields of H_{cric} ~ 3.5 T (critical field) and then the slope gradually becomes negative. Thus according to Banerjee's criteria the transition in the case of $La_{1-x}Ca_xMnO_3$(x~0.83, 0.875) may be considered as second order when the applied magnetic field is below 3.5T [24-26]. The observed second-order nature of the transition can be an intrinsic property of the material. However, the presence of quenched disorder can render a first-order transition to a continuous second-order like transition in the case of doped manganite systems[27]. Under such a situation the observed second-order nature of the transition

can arise due to extrinsic factors, not related to the intrinsic property of the system. This possibility cannot be ruled out for our present samples. Beyond 3.5 T field, the gradual slope change of Arrott plots towards negative value can be attributed to the tendency of a magnetic field induced first order transition and we denote this field as H_{cric} hereafter. Negligible field hysteresis is observed in M(H) curves especially below $H_{cric.}$

The magnetic entropy change (ΔS_M) was calculated from the isothermal M(H) curves using the following Maxwell's equation:

$$\left[\frac{\partial S(T,H)}{\partial H}\right]_T = \left[\frac{\partial M(T,H)}{\partial T}\right]_H \qquad (2)$$

The $-\Delta S_M(T)$ curves for LCMO-1 and LCMO-2 at different magnetic fields (0.1-5T) are shown in Fig.3(a) and its inset. The positive value of ΔS_M below T_N is signature of IMCE due to antiferromagnetic transition[25]. The value of maximum entropy change increases with applied magnetic fields.

In general, the magnetic field dependence of ΔS_M for a magnetic material can be expressed as [17]:

$$\Delta S_M \sim H^n \qquad (3)$$

where 'n' is called a local exponent.

For LCMO-1 and LCMO-2, ln $|\Delta S_M|$ vs. ln H curves are linear (Fig. 3b,c) indicating ΔS_M follows a power law dependence of H according to Eq.3. Interestingly, the value of n is ~ 2 for the entire temperature and magnetic field range (n is calculated from the slope of linear ln ΔS_M vs. ln H plots for different temperatures). In case of FM systems showing CMCE, the value of 'n' is strongly tempera ture dependent [21]. It is ~ 2/3 near the transition temperature (T_C) and ~ 1 well below T_C for a ferromagnetic system. This value reaches '2' at temperatures well above T_C in the paramagnetic regime. In addition, n changes with magnetic field for those materials[17-21]. Thus the magnetic field dependence of ΔS_M is entirely different in the case of an IMCE material in comparison with systems exhibiting CMCE. To better illustrate the magnetic field and temperature dependences of n, we have determined n(H,T) using the formula [19].

$$n = \frac{\mathrm{d} \ln |\Delta S_M|}{\mathrm{d} \mathrm{Ln} H} \qquad (4)$$

It is found that n is ~ 2 (±0.02) regardless of the measurement temperature and magnetic field for both the samples, when the applied field is below H_{cric}. As for example, n(H) for LCMO-1 has been shown in Fig. 3d. However, the value of n becomes ~2 ± 0.1 (fluctuation slightly increases) at applied fields higher than H_{cric} (Fig. 3d). This can be associated with the onset of a magnetic field induced first-order transition. As n is constant in the entire temperature range for magnetic fields, with a very small fluctuation especially below $H_{cric,}$ the normalized ΔS_M (normalized to the value obtained for maximum magnetic field) versus H plots obtained for different temperatures collapse onto the single curve (Fig. 3e, f). The collapse of linear $\ln\left[\frac{\Delta S_M}{\Delta S_{3T}}\right]$ vs. $\ln H$ curves on to a single curve is shown in insets of Fig. 3 e and 3 f for LCMO-1 and LCMO-2, respectively. Consequently $\Delta S_M(T)$ (normalized to maximum value i.e, ΔS_M at antiferromagnetic transition temperature, ΔS_{Max}) for different magnetic fields below H_{cric} can also be collapsed onto a universal curve contrary to the situation in CMCE materials, for which one needs to rescale the temperature axis and define the reference temperature to construct a universal curve. Fig. 3g and 3h show universal $\Delta S_M(T)$ curve for LCMO-1 and LCMO-2 respectively, where the y-axis represents $\Delta S_M/\Delta S_{Max}$ and the x-axis is T/T_N. In this case, we restrict our analysis to the magnetic field range 0.1-3T, which is below the H_{cric}.

To quantify the uncertainty associated with the collapsing of $\Delta S_M(T)$ curves, we have defined a dispersion 'd' corresponding to each point in the universal curve as [23].

$$d = 100 \times \frac{W}{\left(\Delta S_M / \Delta S_{Max}\right)} \qquad (5)$$

where 'W' is the vertical deviation of each entropy curve with respect to its mean value. For both systems, d is found to be less than 6% for most of the points. It has been emphasized in different studies that the measurement uncertainty is always present in indirect measurement of magnetocaloric parameters[28,29]. Pecharsky et al. have quantified measurement uncertainty associated with the calculation of ΔS_M using Maxwell's equation (Eq. 3) as ~ 20 % near transition and it is even higher below a transition temperature[29]. Such kind of measurement uncertainty can give rise to a finite value of d for constructing universal curve[23]. Generally, for the systems showing CMCE, d corresponding to a universal curve is found to be always less than 30% [23]. In our case, d (≤ 6%) is within the reported value obtained for different magnetic

materials. It is even better than the calculated d (~ 9%) for other ferromagnetic manganites published in an earlier work[23].

It should be mentioned that we have also constructed a universal curve including $\Delta S_M(T)$ obtained for magnetic fields beyond H_{cric} (the field range of 0.1-5T). In that case, the obtained maximum d is ~15%, which is well below the typical d associated with universal curves for different materials [23]. Thus the construction of universal curve can be possible for these systems even beyond H_{cric}. As an example, the collapse of $\Delta S_M/\Delta S_{Max}$ vs T/T_N curves for 0.1-5T in the case of LCMO-1 is shown in Fig.4a.

Recently, the large IMCE has been reported in $MnNiGe_{0.915}Al_{0.085}$, which is attributed to a phase transition from hexagonal FM to orthorhombic AFM state[16]. We have checked that a universal curve can also be constructed without rescaling the temperature axis to describe its $\Delta S_M(T)$[16] similar to LCMO-1 and LCMO-2.

From the temperature and magnetic field dependences of these IMCE materials, it can be concluded that IMCE in these antiferromagnetic systems has a unique universal behavior. Unlike the cases of FM systems showing CMCE, the local exponent, n, is independent of temperature and magnetic field for AFM materials, which allows one to construct a universal master curve without rescaling temperature axis as indicated in earlier study [17]. Interestingly, the universal behaviour for these systems, is valid even for the magnetic field induced first order transition.

Now let us discuss the origin of such a different universal behavior of magnetic entropy change for these AFM materials. Since ΔS_M is calculated from the magnetic field dependence of magnetization, we have analyzed the M(H) curves (below H_{cric}) for the present $La_{1-x}Ca_xMnO_3$ samples in the temperature range relevant to IMCE. A parameter ω is defined as $\omega = M/T$. It has been observed that all ω (normalized to its maximum value) versus H curves for a given material can be collapsed onto a single curve as the magnetic field dependence of ω follows a scaling relation: $\omega \sim H^{\xi}$, where ξ is a system-dependent constant. We have evaluated the value of ξ (H,T) by using the following Eq.:

$$\xi = \frac{d \ln |\omega|}{d \, LnH} \qquad (6)$$

For LCMO-1 and LCMO-2, ξ is found to be ~1 (± 0.02) when the field is below H_{cric} and it becomes ~ 1(± 0.1) at the magnetic field higher than $H_{cric.}$ For example, calculated ξ(H,T) for LCMO-1 has been shown in top inset of Fig.4b. The collapsing of the normalized ω versus H curves in the magnetic field range below H_{cric} and in the entire magnetic field range (0-5T) for that sample has been given in Fig.4b and its bottom inset respectively. As ΔS_M is related to M and H via Eq.2, the power law dependence of ΔS_M with magnetic field ($\Delta S_M \sim H^n$ with $n \approx \xi+1$) is easily understood. For these two samples the scaling behavior of ω with H^{ξ} results in their temperature and magnetic field independence of n (≈ ξ+1) and hence the collapsing of $\Delta S_M/\Delta S_{Max}$ versus T/T_N for all different magnetic fields is observed. The estimated value of ξ is almost the same for both LCMO-1 and LCMO-2. Therefore these two samples have nearly the same value of n and their temperature dependences of ΔS_M obtained for different applied fields fall onto the same universal curve inspite of their different chemical compositions and transition temperatures (Fig. 4c). On the other hand, the scaling relation between ω versus H^{ξ} does not exist for FM systems showing CMCE. For those materials, the plot of $M/H^{1/\delta}$ vs. $\varepsilon/H^{-1/(\beta+\gamma)}$ obtained from M(H) curves for different temperatures falls onto a same curve[20,28]. where ε [= $(T-T_C)/T_C$] is called reduced temperature and critical exponents β, γ and δ obey the following relation [30,31]:

$$\beta\delta = \beta + \gamma \qquad (7)$$

Their local exponent n is found to be strongly temperature and field dependent and hence the rescaling of the temperature axis (by introducing T_r) is essential in constructing their universal master curve of $\Delta S_M(T)$ [17-19] .

So far our study focuses only on the AFM compounds, which exhibit IMCE. Therefore one cannot get definite idea about whether the observed universality is related with antiferromagnetic nature of transition or it is a consequence of inverse magnetocaloric property of the materials. To address this issue, we have extended our study in two other types of magnetic systems: (i) systems with the presence of significant AFM correlation in which CMCE occurs and (ii) ferromagnetic systems giving rise to IMCE.

In this regard, we have investigated universal behavior of MCE in case of self-doped $LaMnO_{3.04}$ (LMO). This system shows CMCE with an appreciably large ΔS_M arising due to a magnetic transition from PM to a magnetic state where AFM develops along with FM [9]. Our recent neutron diffraction study confirms the presence of AFM correlations in this material below transition temperature (T_P), which greatly influences its magnetocaloric property [9]. The details of magnetocaloric and magnetic properties of this sample is published elsewhere [9]. In contrary to LCMO-1 and LCMO-2, it appears that the normalized $\Delta S_M(T)/\Delta S_{Max}$ vs. T/T_p (T_p being the temperature corresponding to ΔS_{Max}) plots for different magnetic fields cannot be collapsed onto a universal curve (Fig. 5a) for this compound. The universal curve can be obtained for LMO only when the temperature axis is rescaled, similar to the case of ferromagnetic CMCE systems as proposed by Franco et al.[17] (Fig.5b). From this study, it can be inferred that the construction of a universal curve without rescaling temperature axis can be possible for IMCE materials only. Even for the compounds with AFM correlation showing CMCE, the temperature axis has to be rescaled to construct universal $\Delta S_M(T)$ curve.

Finally, we have analyzed the magnetocaloric data of $Ni_{50}Mn_{36}Sn_{14}$ [14]. It is well established that Ni-Mn-Sn is a ferromagnetic system exhibiting a giant IMCE, due to a first order phase transition from the austensite to martensite state[10]. In particular, $Ni_{50}Mn_{36}Sn_{14}$ undergoes an austensite-martensite transition at ~ 165 K, which is associated with a large IMCE (ΔS_{Max}~ 20 J/kg K for 5T magnetic field) [14]. The magnetic and magnetocaloric properties of this system have been discussed in detail in an earlier study [14]. The temperature dependences of its $-\Delta S_M$ for different magnetic fields are shown in Fig. 6a, which clearly indicates the occurrence of IMCE in the temperature range 150-175 K. We have found that the ΔS_M follows the power law dependence of H ($\Delta S_M \sim H^n$) in the temperature regime associated with IMCE, with a constant exponent n ($\approx 1.1 \pm 0.12$). This is reflected in the collapse of all linear ln $(\Delta S_M/(\Delta S_{5T})$ vs. ln H curves onto a single linear curve (inset, Fig. 6b). As a result, all $\Delta S_M(H)$ curves (normalized to the value at the highest magnetic field, 5T) can be collapsed onto a single curve (Fig. 6b) in the temperature range 150-175 K. In addition to this, all of its $\Delta S_M/\Delta S_{Max}$ vs. T curves also fall onto a universal curve in that temperature range without rescaling the temperature axis (Fig. 6c). The calculated value of maximum d is ~15% in this case. We have also examined the validity of the proposed universal curve for the magnetocaloric data of several other IMCE materials, including

$Ni_{50}Mn_{37}Sn_{13}$ [Ref. 14], $Ni_{49}Pr_1Mn_{37}Sn_{13}$ and $Ni_{47}Pr_3Mn_{37}Sn_{13}$ [Ref. 31], $Ni_{0.5}Mn_{0.35}Sn_{0.15}$ and $Ni_{0.5}Mn_{0.37}Sn_{0.13}$ [Ref. 10], $(Ni,Co)_{50}Mn_{37}Sn_{13}$ (Co~1%) and $(Ni,Fe)_{50}Mn_{37}Sn_{13}$ (Fe~1,3%) [Ref. 32]. These results clearly point out that the construction of a universal curve to describe $\Delta S_M(T)$ without rescaling temperature axis would be a common feature for IMCE materials irrespective of their magnetic states and nature of phase transition. Nevertheless, we note that the validity of the proposed universal behavior may not hold for systems showing a considerable shift in the IMCE peak with magnetic field, such as FeRh [33].

To summarize, we have systematically investigated the temperature and magnetic field dependences of IMCE in different antiferromagnetic and ferromagnetic materials. We find that in contrast to the materials showing CMCE, it is possible to construct a universal master curve to describe $\Delta S_M(T)$ of IMCE systems for different H without rescaling temperature axis. Unlike the case of CMCE, the proposed universal behaviour is found to be valid even when IMCE is associated with the first order phase transition. For such IMCE compounds, ΔS_M follows a power law dependence of magnetic field: $\Delta S_M \sim H^n$, where n is independent of H and T. The construction of a universal curve will be helpful to understand the magnetocaloric response of IMCE materials in any temperature and magnetic field ranges, which would be imperative to judge their prospects in actual magnetic refrigeration devices.

ACKOWLEDGEMENTS:

We acknowledge Prof. V. Franco of Sevilla University for his useful comments. We would like to thank Dr. T. L. Phan and Prof. S. C. Yu of Chungbuk National University for providing the magnetocaloric data of Heusler alloys for verifying our proposed universal behavior. Research at USF was supported by DOE BES Physical Behavior of Materials Program through grant number DE-FG02-07ER46438. Research at SNBNBCS was supported under sponsored unit UNANST-II of the DST, India. MHP acknowledges the support from the Florida Cluster for Advanced Smart Sensor Technologies (FCASST).

REFERENCES

1. K A Gschneidner Jr., V K Pecharsky and A O Tsokol, Rep. Prog. Phys., **68**, 1479 (2005)
2. V. Franco, J.S. Blazquez, B. Ingale, A. Conde, Annu. Rev. Mater. Res, **42**, 305 (2012)
3. M. H. Phan, S. C. Yu, J. Magn. Magn. Mat., **308**, 325 (2007)
4. K.G. Suresh, Phys.Exp., **2**, 18 (2012)
5. N. A. De Oliveira, P. J. Von Ranke, Phys. Rep. **489**, 89 (2010)
6. Anis Biswas, T. Samanta, S. Banerjee, and I. Das, Appl. Phys. Lett., **92**, 212502 (2008)
7. M.H. Phan, M.B. Morales, N.S. Bingham, H. Srikanth, C.L. Zhang and S.W. Cheong Phys. Rev. B, **81**,094413 (2010)
8. T. Samanta, I. Das, S. Banerjee, J.Appl.Phys., 104, 123901 (2008)
9. Sayan Chandra, Anis Biswas, Subarna Datta, Barnali Ghosh, V. Siriguri, A. K. Raychaudhuri, M. H. Phan, H. Srikanth, J. Phys.:Cond.Mat., **24**, 366004 (2012)
10. T. Krenke, E. Dumn, M. Acet, E. Wassermann, X. Moya, L. Manosa, A. Planes, Nat. Mater., **4**, 450 (2005)
11. W.J. Hu, J. Du, B. Li, Q. Zhang, Z. D. Zhang, Appl. Phys.Lett., **92**, 192505 (2005)
12. Anis Biswas, T. Samanta, S. Banerjee, I. Das, Appl. Phys. Lett., **94**, 233109 (2009)
13. S. Chatterjee, S. Giri, S. Majumdar, S. K. De, J. Phys. D: Appl. Phys., **42**, 065001 (2009)
14. T.-L Phan, P. Zhang, N. H. Dan, N. H. Yen, P. T. Thanh, T. D. Thanh, M. H. Phan, S. C. Yu, Appl. Phys. Lett., **101**, 212403 (2012)
15. T. L. Phan, N. H. Duc, N. H. Yen. P. T. Thanh, N. H. Dan, P. Zhang, S. C. Yu, IEEE Trans. Magn., **48**, 1381 (2012)
16. T. Samanta, I. Dubenko, A. Quetz, S. Temple, S. Stadler, N. Ali, Appl. Phys. Lett., 100, 052404 (2012)

17. V. Franco, A. Conde, Int. J. Refr., **33**, 465 (2010)

18. V. Franco, J. S. Blazquez, A. Conde, Appl. Phys. Lett., **89,** 222512 (2006)

19. V. Franco, R. Caballero-Flores, A. Conde , Q . Y. Dong , H. W . Zhang, J. Magn. Magn. Mat., **321**, 1115 (2009)

20. V. Franco, A. Conde, V. K. Pecharsky, K. A. Gschichneidner Jr., Euro. Phys. Lett., **79**, 47009 (2007)

21. M. H. Phan, V. Franco, A. Chaturvedi, S. Stefanoski, G. Nolas, H. Srikanth, Phys. Rev. B, **84**, 054436 (2011)

22. V. Franco, R. Caballero-Flores, A. Conde , Q . Y. Dong , H. W . Zhang, J. Magn. Magn. Mat., **321**, 1115 (2009)

23. C. Marcela Bonilla, J. Herrero-Albillos, F. Bartolome, L. M. Garcia, M. Parra-Borderias, V. Franco, Phys. Rev.B, **81**, 224424 (2010)

24. Anis Biswas, Sayan Chandra, T. Samanta, M. H. Phan, I. Das, H. Srikanth, J. Appl. Phys., **113**, 17A902 (2013)

25. Anis Biswas, T. Samanta, S. Banerjee, I. Das, J. Phys.:Cond.Mat., **21**, 506005 (2009)

26. S. K. Banerjee, Phys. Lett., **12**, 16 (1964)

27. S. Rößler, U. K. Rößler, K. Nenkov, D. Eckert, S. M. Yusuf, K. Dörr, K.-H. Müller, Phys. Rev. B, **70**, 104417 (2004)

28. M. Fodeaki, R. Chahine, T. K. Bose, J. Appl. Phys., **77**, 3528 (1999)

29. V. K. Pecharsky, K. A. Gschneidner Jr., J. Appl. Phys., **86**, 565 (1999)

30. H. Eugene Stanley, *Introduction to Phase Transitions and Critical Phenomena* (Oxford University Press, New York, 1971)

31. B. Widom, J. Chem. Phys., **43**, 3898 (1965)

32. In private communication with S.C. Yu and T.L. Phan.

33. T. Krenke, E. Duman, M. Acet, X. Moya, L. Manosa, A. Planes, J. Appl. Phys., **102**, 033903 (2007)

34. M. P Annaorazov, S A Nikitin, A LTyurin , K A Asatryan, A K Dovletov, J. Appl. Phys., **79** 1689 (1996).

Figure captions:

Fig.1: X-ray diffraction pattern of $La_{0.17}Ca_{0.83}MnO_3$ (LCMO-1) and $La_{0.125}Ca_{0.875}MnO_3$ (LCMO-2). Inset: x-ray diffraction pattern of $LaMnO_{3.04}$

Fig.2: (a) M(H) curves at some selected temperatures for LCMO-1. Inset: M(T) curves for LCMO-1 and LCMO-2. (b) M vs.H curves for LCMO-2 at some selected temperatures. Inset: Arrot plots for that sample at some selected temperatures around transition.

Fig. 3: (a) $-\Delta S_M(T)$ for different magnetic fields ranging 0.1-5T obtained for LCMO-1. There exists clear signature of IMCE at ~ 167 K. Inset: $-\Delta S_M(T)$ measured in same magnetic field ranges for LCMO-2 (b) $\ln|S_M|$ vs $\ln|\mu_o H|$ curves in range 0.1-5T for LCMO-1 at three selected temperatures : at below transition, around transition and above transition respectively. (c) Same curves for LCMO-2. (d) The magnetic field dependence of n (defined as Eq. 4) at different temperatures (0.1-5T) in case LCMO-1. (e) $\Delta S_M(H)$ normalized to its value for 3T field measured at different temperatures ranging 75-250 K collapse into a single curve in case of LCMO-1. Inset: linear $\ln\left[\frac{\Delta S_M}{\Delta S_{3T}}\right]$ vs. $\ln H$ curves at different temperatures collapse onto a single linear curve for the sample (in the field range below H_{cric}). (f) $\Delta S_M(H)$ normalized to its value for 3T field measured at different temperatures collapse into a single curve in case of LCMO-2. Inset: linear $\ln\left[\frac{\Delta S_M}{\Delta S_{3T}}\right]$ vs. $\ln H$ curves at different temperatures fall on to a single curve for the sample. (g) Universal $\Delta S_M(T)/\Delta S_{Max}$ versus T/T_N for LCMO-1 obtained at different magnetic fields below $H_{cric.}$ (h) same curve for LCMO-2.

Fig.4: (a) $\Delta S_M(T)/\Delta S_{Max}$ versus T/T_N obtained for entire temperature range (0.1-5T) in case of LCMO-1. (b) ω/ω_{max} versus H for different temperatures (70-250 K) fall into a single curve for LCMO-1 when magnetic field is below H_{cric} (0-3T). Here ω_{max} is the value of ω at 3T magnetic field. Top inset: magnetic field dependence of ξ (calculated using Eq. 6) at different

temperatures. Bottom inset: ω/ω_{max} versus H in entire temperature range. The value of ω at 5T magnetic field is taken as ω_{max} (c) $\Delta S_M(T)/\Delta S_{Max}$ versus T/T_N curves for all different magnetic fields collapse onto same universal master curve in cases of both LCMO-1 and LCMO-2.

Fig.5: (a) $\Delta S_M(T)$ curves obtained at different magnetic fields for $LaMnO_{3.04}$ (LMO) (b) $\Delta S_M(T)/\Delta S_{Max}$ versus T/T_P [T_P being temperature corresponding to the peak of $\Delta S_M(T)$] curves measured for different magnetic fields do not fall onto same curve in case of $LaMnO_{3.04}$ (LMO). (c) $\Delta S_M(T)/\Delta S_{Max}$ curves collapse onto universal curve for LMO when temperature axis is rescaled according to equation (1).

Fig.6: (a) Temperature dependence of ΔS_M for different magnetic field (1-5T) in the case of $Ni_{50}Mn_{36}Sn_{14}$ (NMS). (b) $\Delta S_M(H)$ curves normalized to its value for 5T field measured at different temperatures ranging between ~150 and 175 K collapse onto a single curve for the sample. Inset: linear $\ln\left[\frac{\Delta S_M}{\Delta S_{3T}}\right]$ vs. $\ln H$ curves at different temperatures within that temperature range collapse onto a single linear curve. (c) $\Delta S_M(T)/\Delta S_{Max}$ versus T/T_P [T_P is the temperature corresponding to the inverse magnetocaloric peak of $\Delta S_M(T)$] curves measured at different magnetic fields fall onto a universal curve for the sample.

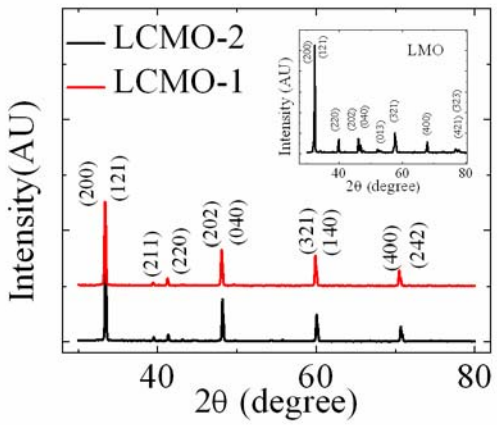
LCMO-2
LCMO-1
Intensity(AU)
(200)
(121)
(211)
(220)
(202)
(040)
(321)
(140)
(400)
(242)
40
60
80
2θ (degree)
LMO
Intensity (AU)
(200)
(121)
(220)
(202)
(040)
(013)
(321)
(400)
(421)
(323)
40
60
80
2θ (degree)

Fig. 1

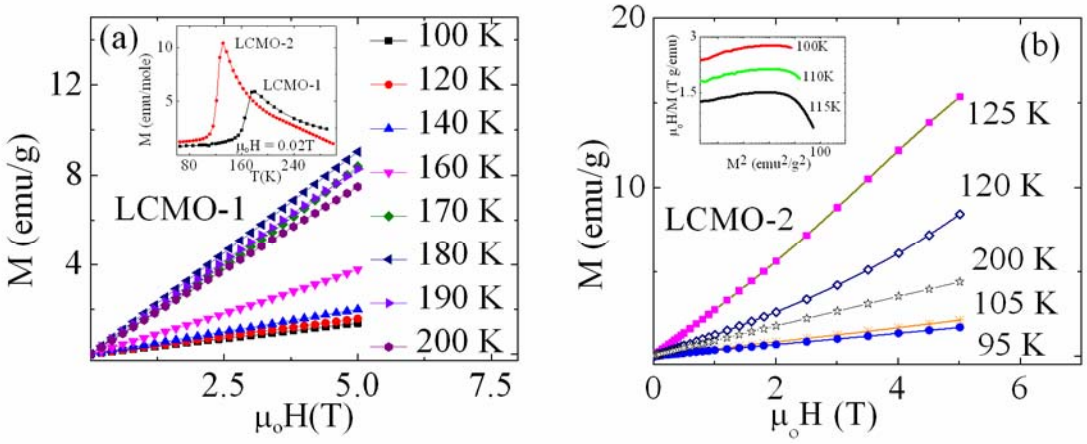
(a)
LCMO-1
LCMO-2
LCMO-1
μ_oH = 0.02T
M (emu/mole)
T(K)
100 K
120 K
140 K
160 K
170 K
180 K
190 K
200 K
M (emu/g)
μ_oH(T)
(b)
LCMO-2
100K
110K
115K
μ_oH/M (T g/emu)
M^2 (emu^2/g^2)
125 K
120 K
200 K
105 K
95 K
M (emu/g)
μ_oH (T)

Fig. 2

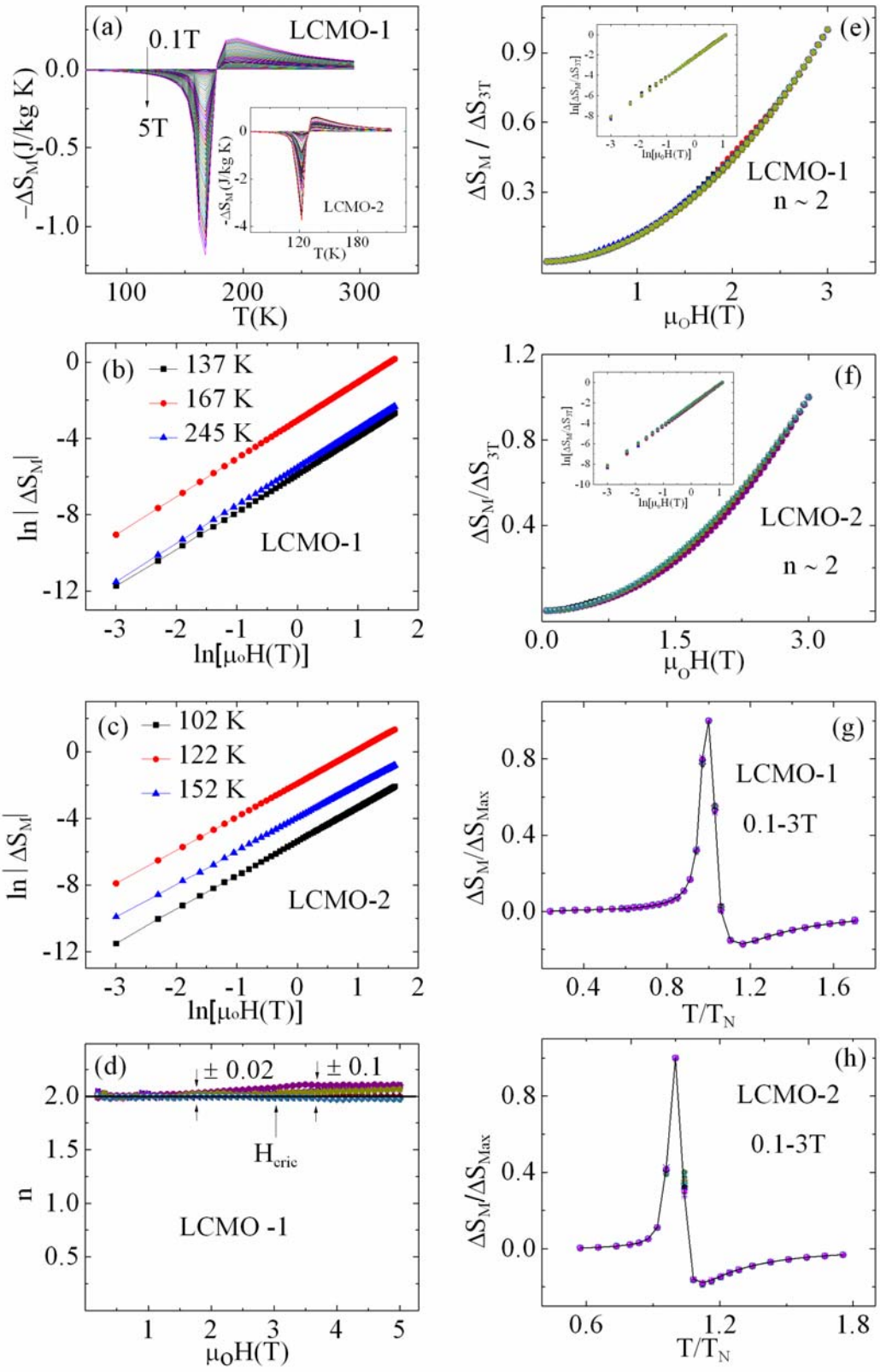
(a)
0.1T
5T
LCMO-1
LCMO-2
$-\Delta S_M$(J/kg K)
T(K)
(b)
137 K
167 K
245 K
LCMO-1
$\ln|\Delta S_M|$
$\ln[\mu_o H(T)]$
(c)
102 K
122 K
152 K
LCMO-2
(d)
± 0.02
± 0.1
H_{crie}
LCMO -1
n
$\mu_O H(T)$
(e)
LCMO-1
n ~ 2
$\Delta S_M / \Delta S_{3T}$
(f)
LCMO-2
n ~ 2
(g)
LCMO-1
0.1-3T
$\Delta S_M/\Delta S_{Max}$
T/T_N
(h)
LCMO-2
0.1-3T

Fig. 3

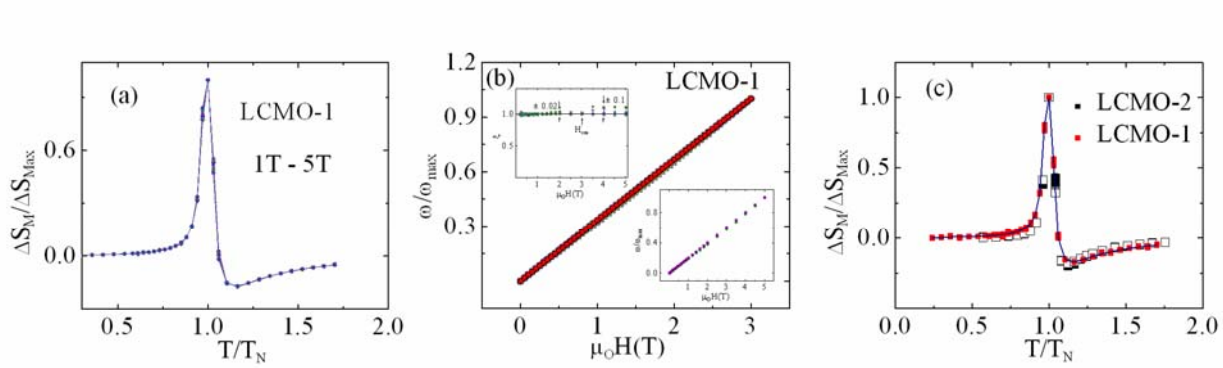
(a)
LCMO-1
1T - 5T
$\Delta S_M/\Delta S_{Max}$
T/T_N
(b)
LCMO-1
ω/ω_{max}
$\mu_O H(T)$
(c)
LCMO-2
LCMO-1
$\Delta S_M/\Delta S_{Max}$
T/T_N

Fig. 4

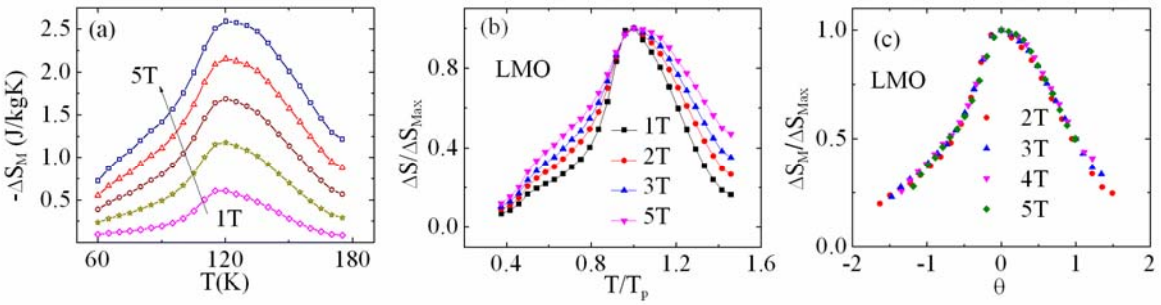
(a)
5T
1T
$-\Delta S_M$ (J/kgK)
T(K)
(b)
LMO
1T
2T
3T
5T
$\Delta S/\Delta S_{Max}$
T/T_p
(c)
LMO
2T
3T
4T
5T
$\Delta S_M/\Delta S_{Max}$
θ

Fig. 5

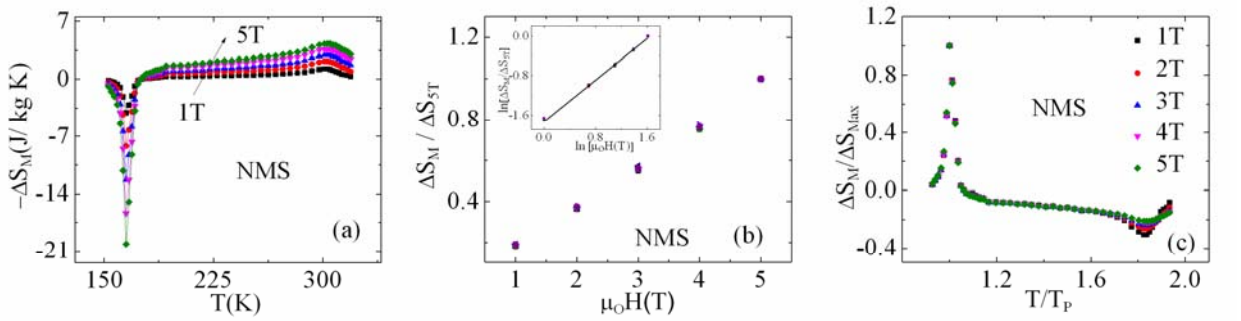
7
0
-7
-14
-21
$-\Delta S_M$(J/ kg K)
5T
1T
NMS
(a)
150
225
300
T(K)
1.2
0.8
0.4
ΔS_M / ΔS_{5T}
NMS
(b)
1
2
3
4
5
μ_OH(T)
1.2
0.8
0.4
0.0
-0.4
$\Delta S_M/\Delta S_{Max}$
NMS
1T
2T
3T
4T
5T
(c)
1.2
1.6
2.0
T/T_P

Fig. 6